The Influence of Alkyl-Chain Length on Beta-Phase Formation in Polyfluorenes

By *Daniel W. Bright, Fernando B. Dias, Frank Galbrecht, Ulli Scherf,* and *Andrew P. Monkman**

Di-*n*-alkyl substituted polyfluorenes with alkyl chain lengths of 6, 7, 8, 9, and 10 carbon atoms (PF6, PF7, PF8, PF9, and PF10) are studied in dilute solution in MCH using optical spectroscopy. Beta-phase is formed upon cooling in solutions ($\sim 7\ \mu g\ mL^{-1}$) of PF7, PF8, and PF9 only, which is observed as an equilibrium absorption peak at ~ 437 nm and strong changes in the emission spectra. Beta-phase is formed upon thermal cycling to low temperature in solutions ($\sim 7\ \mu g\ mL^{-1}$) of PF7, PF8, and PF9, which is observed as an equilibrium absorption peak at ~ 437 nm and strong changes in the emission spectra. Beta phase is found to occur more favorably in PF8 than in PF7 or PF9, which is attributed to a balance between two factors. The first is the dimer/aggregate formation efficiency, which is poorer for longer (more disordered) alkyl chain lengths, and the second is the Van der Waals bond energy available to overcome the steric repulsion and planarize the conjugated backbone, which is insufficient in the PF6 with a shorter alkyl chain. Beta phase formation is shown to be a result of aggregation, not a precursor to it. A tentative value of the energy required to planarize the fluorene backbone of (15.6 ± 2.5) kJ mol^{-1} monomer is suggested. Excitation spectra of PF6, PF7, PF8, and PF9 in extremely dilute (~ 10 ng mL^{-1}) solution show that beta phase can form reversibly in dilute solutions of PF7, PF8 and PF9, which is believed to be a result of chain collapse or well dispersed aggregates being present in solution from dilution of more concentrated solutions. PF7, PF8, and PF9 also form beta phase in thermally cycled solid films spin-cast from MCH. However, in the films the PF7 formed a larger fraction of beta phase than the PF9, in contrast to the case in solutions, because it is less likely that the close-packed chains in the solid state will allow the formation of planarized chains with the longer PF9 side chains.

1. Introduction

The phase behavior of alkyl-substituted polyfluorenes, especially poly(9,9-di-*n*-octylfluorene) (PF8), has a significant effect on their emission properties,[1–5] and there have been many reports directed towards understanding the nature and microscopic structure of these phases,[2,3,6–12] which is driven by the strong suitability of polyfluorenes for light emitting device applications, because of their thermal and chemical stability, color tunability, and high fluorescence efficiency.[13–16] In particular, there is a sharp, red-shifted absorption peak observed in PF8 at 437 nm, which can be induced by thermal processing,[3,6,17] and has been attributed to the presence of beta phase (the C_β isomer).[17,18] This phase is also present in both solutions of PF8 in poor solvents and in thin films exposed to solvents.[8,17,19] It can strongly affect the emission spectrum even in low quantities, by acting as a low energy trap for excitons generated within the alpha phase bulk,[4,5,16,17] and can even give rise to efficient ASE.[20]

The beta phase in PF8 has been studied intensively with the objective of understanding its microscopic structure, including a study of oligomers.[21] X-ray and neutron scattering have been employed to study the physical structure of the polymer chains in films,[2,3,12] and solutions,[9,10,22,23] including the study of a family of similar polymers with different alkyl chain lengths: poly(9,9-di-*n*-hexlyfluorene) (PF6), poly(9,9-di-*n*-heptylfluorene) (PF7), poly(9,9-di-*n*-octylfluorene) (PF8), and poly(9,9-di-*n*-nonylfluorene) (PF9), and poly(9,9-di-*n*-decylfluorene) (PF10). The polymers PF7, PF8, and PF9 (and to some extent, PF6) were found to contain sheet-like structures in solution in methylcyclohexane (MCH), a poor solvent. These are thought to be the precursors to beta phase aggregates. Beta phase emission was found in MCH solutions of PF7, PF8, and PF9, but not PF6 or PF10.[10]

In this paper, the same family of polyfluorenes is studied in solution in MCH, using optical spectroscopy to show the trend in the formation of beta phase with alkyl chain length. The equilibrium component of beta phase in these polymer solutions

[*] Prof. A. P. Monkman, D. W. Bright, Dr. F. B. Dias
Organic Electroactive Materials Group
Department of Physics, University of Durham
South Road, Durham, DH1 3LE (UK)
E-mail: a.p.monkman@dur.ac.uk; d.w.bright@dur.ac.uk
F. Galbrecht, Prof. U. Scherf
Bergische Universität Wuppertal
Institut für Polymertechnologie
Makromolekulare Chemie
Gauss-Str. 20, 42097 Wuppertal (Germany)

DOI: 10.1002/adfm.200800313

is studied as a function of temperature, showing that the formation of beta phase is most favorable specifically for the octyl-substituted PF8. Excitation spectra and emission spectra show the reversible formation of beta phase even in extremely dilute solutions of the polymers PF7, PF8, and PF9. Finally, beta phase formation was demonstrated in thermally cycled spin-cast films of PF7, PF8, and PF9.

2. Results

All the absorption spectra shown in Figure 1 were obtained after reaching equilibrium at each temperature. MCH is a poor solvent for polyfluorenes and precipitation can occur upon reducing the temperature, even at quite low concentrations.[17] However, data collected using very dilute samples is unaffected by this, and an isobestic point could be clearly seen in the absorption spectra of PF8 taken as a function of temperature.[17] The curves at lower temperatures were normalized at the isobestic point identified previously in PF8,[17] to correct for precipitation effects.

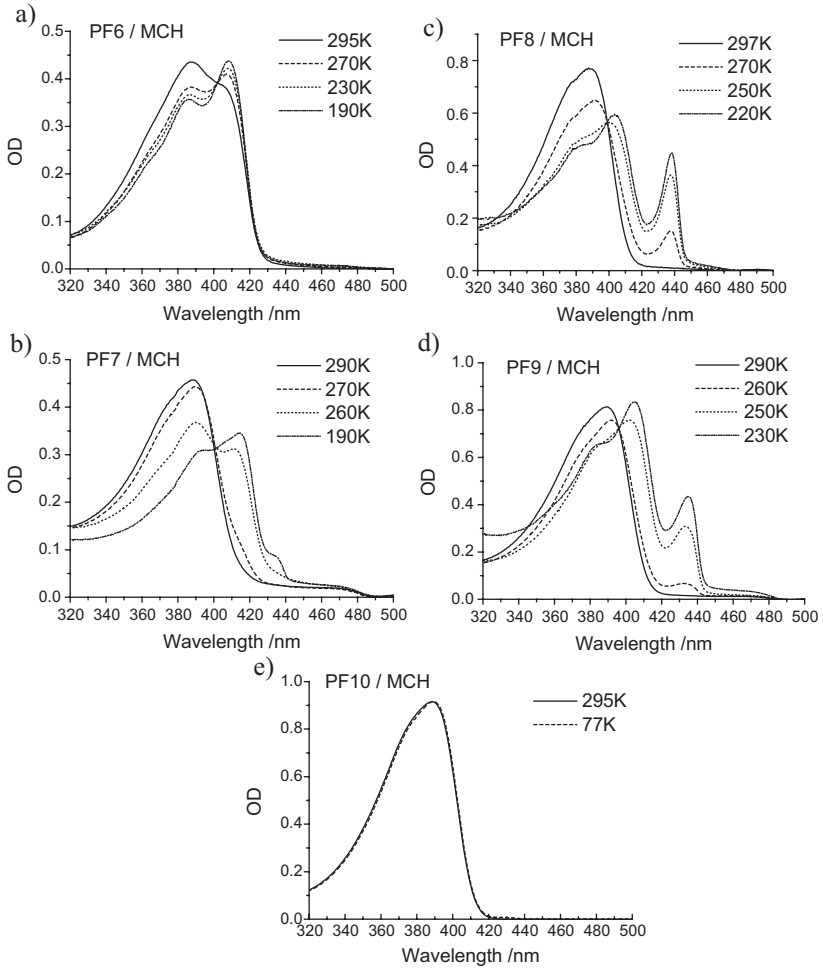

Figure 1. Temperature dependent absorption spectra for the polyfluorenes a) PF6 (6 μg mL^{-1}), b) PF7 (6 μg mL^{-1}), c) PF8 (23 μg mL^{-1}), d) PF9 (7 μg mL^{-1}) and e) PF10 (10 μg mL^{-1}).

In PF6 at room temperature, the main band shows a peak at 387 nm and a shoulder at 408 nm. This 408 nm shoulder dominates over the peak at lower temperatures, but no peak corresponding to the presence of beta phase is observed at ~437 nm. In PF7 the main band is red-shifted significantly by the appearance of a new peak at 414 nm, and a small shoulder around 435 nm indicates the formation of beta phase in this polymer at very low temperatures. Note that this new absorption band starts to be observed only below 200 K and no further growth is detected down to the freezing point of the solvent (160 K). The PF8 main band is redshifted by a new peak appearing at 408 nm, and a strong absorption band at 437 nm which appears below 280 K and grows stronger with decreasing temperature. PF9 shows very similar behavior to PF8; a new main band absorption appears at 405 nm, along with strong absorption at 434 nm, similar to that seen in the PF8 but of lower height relative to the main absorption band. PF10 shows no change in absorption spectrum even at low temperatures.

Figure 1 clearly shows that the length of the linear alkyl side chain is a strong influence on the formation of beta phase, and that formation is most favorable for (but not restricted to) a chain length of 8 carbon atoms. The decrease in solvent action at lower temperatures, with concomitant increase in polymer-polymer interaction, is not sufficient to explain this favorability. In fact, PF6 is affected the most by solvent action because it is the least soluble of the polymers, yet no beta phase is observed.

PF6 shows interesting behavior when stored at room temperature. After heating to 100 °C, the spectrum is the same as that of the PF10, but over the course of 6 hours at 295 K the absorption spectrum spontaneously shifts to become structured (Fig. 2a), indicating the presence of an aggregate. The presence of an aggregate is supported by the data in Figure 2b, where the first larger aggregates formed (when the solution is more concentrated) are seen to drop out of the stirred solution after 100 minutes, and the remainder of the smaller aggregates are kept suspended by the stirring. Such structured absorption is not seen in solutions of poly(9,9-di(ethylhexyl)fluorene) (PF2/6) in MCH,[24] which has branched side chains. This structure in the main absorption band, which becomes more pronounced upon cooling, is very similar to the low temperature structure in the absorption spectra of PF7, PF8, and PF9 (Fig. 1a–d), indicating that they too are forming aggregates. This data is consistent with previous structural studies by Knaapila et al.[10] which found sheet-like aggregates formed by PF6, PF7, PF8, and PF9 but not PF10.

Fluorescence spectra are far more sensitive than absorption spectra, and can be used to investigate the reversibility of beta phase formation in very dilute solutions (~10 ng mL^{-1}) in order to avoid as far as possible the effects of aggregation and precipitation. Figure 3

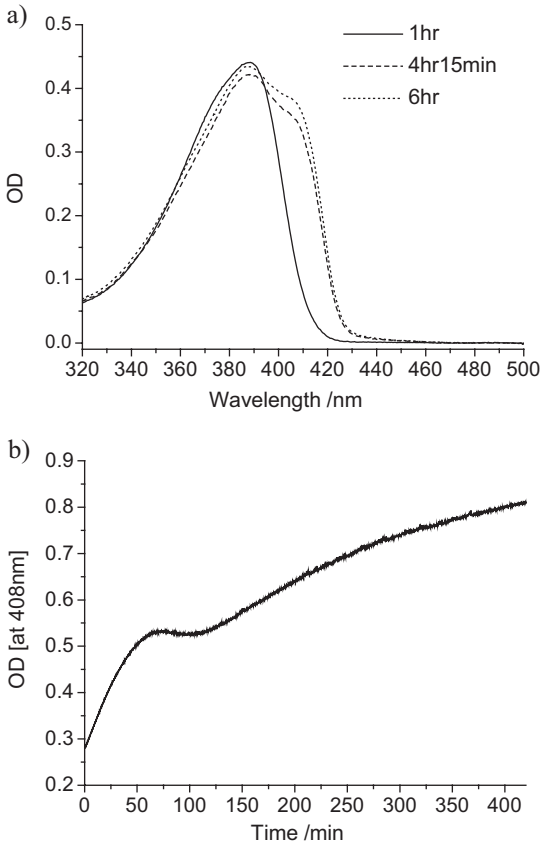

Figure 2. a) The absorption spectrum of (6 μg mL^{-1}) PF6/MCH, taken at intervals after boiling the solution then returning to 295K. b) The absorption at 408 nm of a magnetically stirred 20 μg mL^{-1} solution of PF6/MCH as a function of time.

shows excitation spectra with emission collected at 460 nm. For each sample, an excitation spectrum was initially collected at 295 K, then it was cooled sufficiently to induce beta phase formation, and a second spectrum was taken. Then the sample was returned 295 K and spectra were recorded as a function of time. The sharp peak observed at 404 nm is due to Raman scattering from the solvent. The spectra for all the solutions and especially PF6 show that the main absorption band drops to below their original levels, and in the case of PF6 the signal almost disappeared after 24 h. The signal was not restored upon boiling of the solutions, which would have indicated that the drop in signal was due to precipitate falling to the bottom of the cuvette. The reason for this loss is not clear, but it is likely to be either photodegradation, because the samples were tested repeatedly and so were continuously subject to intense UV and blue light, or adsorption onto the cuvette walls, which is likely to occur after such an extended duration. However, the results agree completely with those in the absorption spectra in Figure 1.

The PF6 does not display any beta phase peak even at 190 K, which is concurrent with the absorption spectrum in Figure 1a. The initial spectrum at 295 K (Fig. 3a) appears blue-shifted with respect to the equilibrium absorption, as the sample was only left at 295 K for ~1.5 hours before taking the first excitation spectrum and cooling, whereas 6 hours are required to reach equilibrium (Fig. 2). The data after cooling are then fully consistent. The PF7 spectrum at 200 K shows the same shoulder that is seen in its absorption (Fig. 3b), as well as the red-shifting of the main band. The beta phase shoulder disappears almost entirely within an hour of returning to 295 K, but the red-shifted shoulder returns to the original profile over a much longer timescale; it has still not fully recovered after 48 h. The PF8 (Fig. 3c) shows a very large peak at 438 nm, which is still present after 24 h, but dropping with respect to the main band peak height. There is a remnant of the peak (not shown in the figure for clarity) remaining after 40 h, in contrast to the results from Dias et al. visible due to the lower noise in this new data. In the PF9 at 220 K, there is again a good reproduction of the absorption spectrum profile (Fig. 3d), with a strong absorption band at 430 nm attributed to the beta phase, and a main band red-shift. Both of these changes return back to the original profile at 295 K within 48 h, and both changes occur over similar timescales.

The emission spectra (Fig. 4) were recorded in tandem with the excitation spectra, and show the same degradation in signal over extended measurement times that is seen in those tests for PF9 and PF6. The PF6 emission spectra show an interesting red-shift of the whole spectrum at 190 K, with the short wavelength peak moving from 413 nm to 424 nm. Upon returning to 295 K, this peak shifts back slightly to 420 nm after an hour and to 418 nm after ~24 h. In the PF7, PF8, and PF9 spectra, there is a sharply defined peak of emission at 437–438 nm, and the broad 413 nm emission peak that dominates at 295 K is suppressed. This change is fully reversible within one day.

Solid-state films of these polyfluorenes were spin-cast from MCH (10 mg mL^{-1}) and cooled to well below the transition temperature (in the region of 160 K), then slowly warmed to 290 K at a rate of 0.6 K min^{-1}. The resulting emission spectra are shown in Figure 5. In the solid state PF6 does not form any beta phase, in concordance with the solution sample results. The emission is characteristic of the amorphous phase, broadened and slightly red-shifted with respect to the initial emission spectra at 295 K in Figure 4b, and does not change after the thermal cycle. In PF7, an intense, sharp beta phase emission peak is produced at 436 nm after the thermal cycle, and the final spectrum is very similar to the low temperature emission spectrum of PF7 in Figure 4b. The initial spectrum of the PF8 film shows emission entirely dominated by the beta phase, which peaks at 441 nm. This emission is greatly enhanced by the thermal cycle. In the PF9, the final spectrum shows a small sharp beta phase emission peak overlaid onto a predominantly amorphous phase emission spectrum, indicating the formation of a very small fraction of beta phase in the sample, given the efficient transfer of excitons to the beta phase.[4,5,16,17]

3. Discussion

The temperature dependant absorption spectra show that PF6 does not exhibit the red-shifted peak in the region of 437 nm that is attributed to the formation of beta phase. The polymer spontaneously aggregates at room temperature, and main absorption band at equilibrium is composed of two peaks at 387 nm and 408 nm, the first of which dominates at 295 K. These

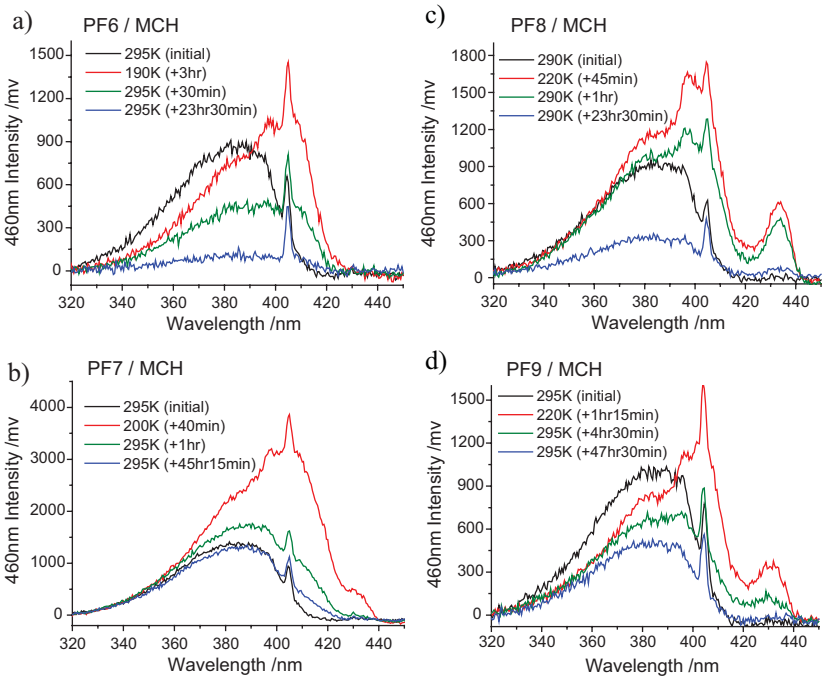

Figure 3. Excitation spectra of a) PF6, b) PF7 c) PF8 and d) PF9 dilute solutions in MCH during a cooling – warming cycle. All solutions were of concentration ~10 ng mL^{-1}. Spectra were recorded as follows: at 295 K; after cooling to sufficiently low temperature to induce beta phase formation; as a function of time after warming back to 295 K. The sharp spike at 404 nm is the Raman peak of the MCH.

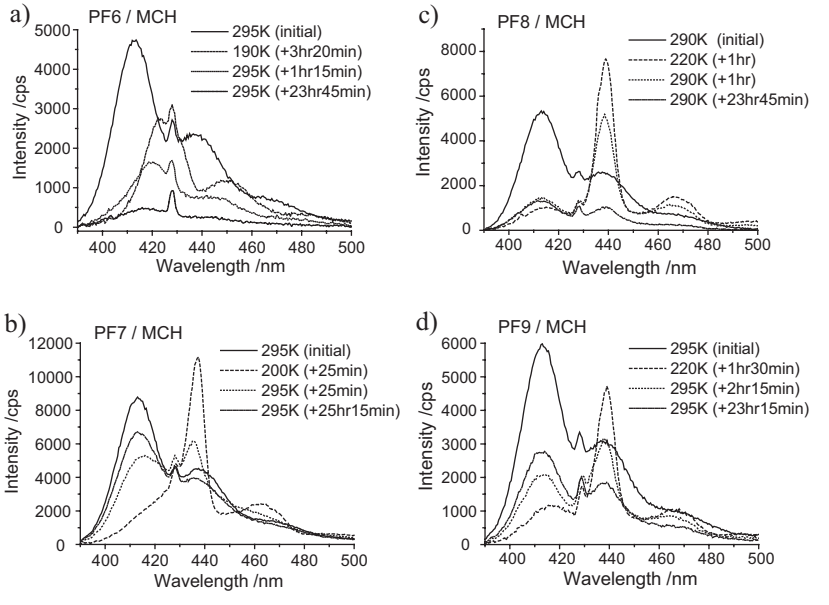

Figure 4. Emission spectra of a) PF6, b) PF7 c) PF8 and d) PF9 dilute solutions in MCH. Spectra were recorded as follows: at 295 K; after cooling to sufficiently low temperature to induce beta phase formation; as a function of time after warming back to 295 K. The sharp spike at 428 nm is the Raman peak of the MCH.

peaks exchange intensity as the sample is cooled, such that the longer wavelength peak dominates at 190 K. This indicates the presence of an aggregate which forms even at 295 K, leading to structure in the emission.

Figure 6 represents the evolution with temperature of the beta phase peak intensity in PF8 and PF9, normalized to the maximum value (β_{max}) observed at low temperatures. With this definition, the ratio $\beta/\beta_{max} = 0$ at 295 K, and $\beta/\beta_{max} = 1$ at the lower temperature. This allows the concentration dependence and the onset temperature to be more easily perceived. Note that a second analysis was carried out on one dataset using the relative areas of the beta phase peaks, which gave identical results within the error of the data.

First, the data for PF8 are independent of concentration over the range studied, with an onset around 275 K. This is in line with previous observations.[9,22] It is normally the case that for emission from aggregates that the data here would be concentration dependent. However, even though the beta phase is formed through an aggregation process, the emission is produced from the same number of non-interacting polymer chains as before the aggregation process; it is not excimer emission. Although the alkyl side chains of adjacent backbone chains are interacting, this only serves to planarize the fluorene units. The emitting chromophores are not interacting with each other; hence no concentration dependence is present.

The PF9 has a lower onset temperature at 265 K, indicating that the beta phase requires lower temperature to form and is therefore formed less easily in this polymer compared to PF8. For PF7, the data cannot be analyzed in such a way because of the increase in the 435 nm background signal at 260 K (Fig. 1b), which would give a false indication of the onset temperature from the background shift rather than the true onset given by the appearance of the shoulder. This masks the actual height of the beta phase peak, and the only clear conclusions that can be drawn are that the onset is around 200 K, which is taken to be the point where the shoulder appears, and that the peak heights are the same at 190 K and 180 K, indicating that the formation reaches saturation by 190 K. This is sufficient evidence to indicate that the formation of beta phase is a less efficient process in PF7 than in both PF8 and PF9.

The absorption spectra of PF7, PF8, and PF9 also show a red-shifting of the main absorption band as the temperature is lowered, as a result of the appearance of a new absorption peak at

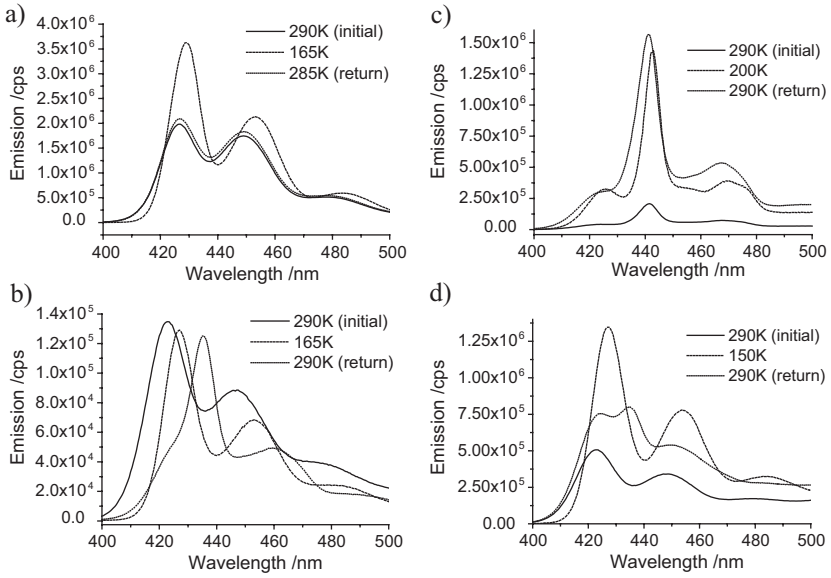

Figure 5. The emission spectra of a) PF6, b) PF7 c) PF8 and d) PF9 films spin-cast from 10 mg mL^{-1} in MCH. The samples were then cooled, and reheated to room temperature at a rate of 0.6 K min^{-1}.

the expense of the original dominant absorbing peak. This strongly suggests the formation of an aggregate in the same manner as the PF6, but at lower temperatures. These aggregates have been found in previous work.[10] No such aggregate appears in PF10. The four shorter chain polymers form an aggregate, but the beta phase is only detected in the spectra of PF7, PF8, and PF9.

The following model is proposed for the behavior of this family of polymers. In poor solvent, PF8 forms sheet-like aggregates, with interdigitated alkyl chains holding the polyfluorene backbones together in the aggregate, as described in the scheme by Knaapila et al.[10] This leads to the structure of the main band absorption, with a peak near 408 nm. The binding energy from the Van der Waals bonding in the alkyl chains is sufficient to overcome the steric hindrance of the polyfluorene backbone and planarize it, leading to a further red-shifted absorption at 437 nm. Brinkmann also concluded that interdigitation of side chains is a prerequisite to crystallization of PF8.[11]

Similar changes occur in the PF7 and PF9, although in the PF7 the Van der Waals bond energy from the shorter chains is barely sufficient to planarize the polymer backbone, and in the PF9 the alkyl chains are longer and more disordered, giving rise to weaker bonding and hence less beta phase formation than is observed in PF8. In the PF6 the short alkyl chains do not provide sufficient energy to overcome the steric hindrance, and so strong aggregate absorption is seen at 408 nm, but there is no beta phase absorption. SANS and SAXS data show no difference between the structure of the PF6 and PF8 aggregates,[10] but the only difference between them is that of the backbone torsion angles, which is too subtle a difference to pick up from scattering data. In the PF10, the alkyl chains are too long and disordered to allow stable aggregate formation, as even at low temperatures the disordered motion of the alkyl chains is enough to prevent aggregation.

In the films, the beta phase forms less effectively than in solution, because there is less freedom to move and form the interdigitated structure, and the presence of closely packed chains further inhibits the backbone planarization. Interestingly, the PF7 film forms a larger fraction of beta phase than PF9 after thermal cycling, shown by the relatively larger characteristic emission peak in Figure 5. It is less likely that the close-packed chains in the solid state will allow the formation of planarized chains with the longer side chains in the PF9.

A differential scanning calorimetry (DSC) study was carried out by Miyahara et al. into the enthalpy of melting of alkyl side chains in alkyldiethylamines.[25] They found a consistent phase transition from the dissociation of the alkyl side chains, with a clear linear dependence of the enthalpy on the alkyl chain lengths of 10 to 18 carbon atoms. This data was extrapolated back to 6 carbon atoms, and compared to a DSC study of the dissociation energy of PF8 by Kitts et al.[22] The data and projections are shown in Figure 7, and show good agreement. The borderline beta phase formation in PF7, taking into account the uncertainty in the extrapolation, suggests a tentative value of (15.6 ± 2.5) kJ mol^{-1} monomer for the energy required to planarize the fluorene units.

The difference in low temperature and room temperature absorption spectra for PF6, PF7, PF8 and PF9 are shown in Figure 8. The PF8 difference spectrum clearly shows two positive peaks at 409 nm and 437 nm, which Dias et al. attributed to the absorption and 0–1 vibronic of the beta phase.[17] However, the first peak is also present in the PF6 absorption spectrum, which shows no beta phase absorption or emission, and so the first peak is now re-assigned to be the result of the aggregate absorption rather than the beta phase absorption.

The excitation spectra of PF6, PF7, PF8, and PF9 in very dilute solutions in MCH largely mirror their absorption spectra in more

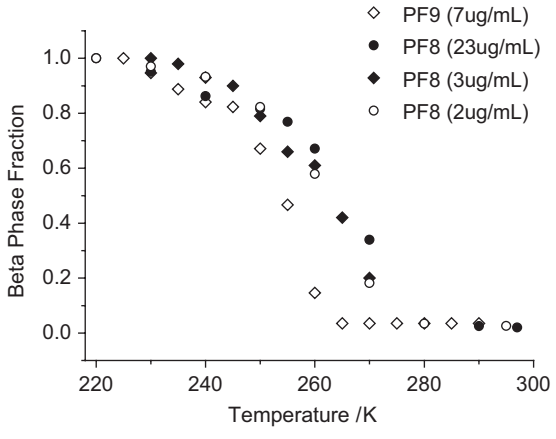

Figure 6. The relative fraction of beta phase present in each sample as a function of temperature. Error bars are ~twice the point size.

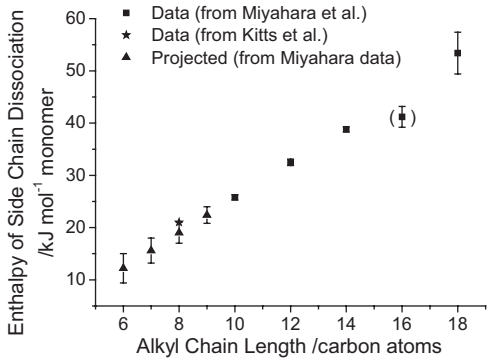

Figure 7. The enthalpy of dissociation of different alkyl chain lengths from studies by Miyahara et al. and Kitts et al. and the projected enthalpies for chain lengths of 6, 7, 8 and 9 carbon atoms.

concentrated solutions. At low temperatures, there is a peak formed in the PF8 and PF9 spectra and a shoulder in the PF7 spectrum that match the beta phase peaks in their absorption counterparts, and beta phase is again not seen in PF6. The spectra as a function of time (after returning to 295 K) show that the peaks indicating the presence of beta phase in the samples disappear within 2 h for the PF7, ~40 h for PF8 and 6 h for the PF9. This is consistent with the graph in Figure 4 showing that the beta phase forms most efficiently in PF8, then less efficiently in PF9 and poorly in PF7. However, in PF6 and PF7 the red-shifted main band peak that appears in the excitation spectra recovers over a far longer timescale of several days. This indicates that the aggregation producing this emission is different to the formation of beta phase, and far more stable. The red-shifted main band peak in PF8 and PF9 recovered at the same rate as the beta phase peak, indicating that the aggregate in PF6 and PF7 is more stable than in the PF8 and PF9, which is consistent with the relatively lower solubility of the PF6 and PF7.

The temperature dependent emission spectra of PF6, collected concurrently with the excitation spectra, show anomalous behavior when compared to those of the PF7, PF8, and PF9.

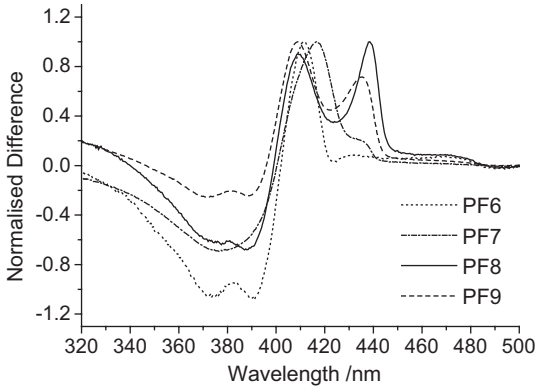

Figure 8. The normalized difference spectra of PF6, PF7, PF8 and PF9, obtained by subtracting the room-temperature absorption spectra (in solution) from the low-temperature absorption spectra.

In PF7, PF8, and PF9, the main broad emission peak of 413 nm at 295 K is suppressed at low temperature in favor of a sharp emission peak at 437–438 nm due to the presence of beta phase. This change is reversible over similar (but slightly longer) timescales to the disappearance of the beta phase peaks in the excitation spectra of the samples. This discrepancy is due to the migration of emissive excitons favoring the lower energy emissive state of the beta phase,[4] so that small remnants of beta phase that cannot be detected in the absorption spectra can still contribute significantly to the emission spectrum. In the PF6, there is no quenching of the 413 nm emission peak, but the whole emission spectrum appears to be redshifted by ~11 nm by the formation of larger aggregates at lower temperature, as indicated by the increasing structure in the absorption at lower temperature (Fig. 1a). This is consistent with no beta phase being formed, as there is no sharp emission peak or quenching of the other peaks.

For the polymers which displayed a beta phase peak, the beta phase formation was detected even at extremely low concentrations (~10 ng mL^{-1}). This is consistent with the more concentrated solutions if the solutions contain well dispersed aggregates (passed on from the more concentrated original source solutions) or folding up of the long individual chains.

4. Conclusions

PF7 and PF9 display similar behavior to PF8 in the formation of a reversible beta phase transition in dilute solutions in MCH. The transition to the beta phase, observed through changes in absorption spectra, occurs at lower temperatures for the PF7 (~200 K) and PF9 (265 K) than PF8 (275 K). The maximum intensity of the beta phase absorption is also lower in the PF7 and PF9 than it is in PF8, indicating that PF8 has an optimal side chain length for the formation of this phase. The formation of beta phase is found to be a result of aggregation, which occurs in PF6, PF7, PF8, and PF9, but the beta phase is formed only if the side chain interactions are stable and sufficient to overcome the steric repulsion and planarize the polymer backbone; hence no beta phase is formed in the PF6, although it spontaneously aggregates at room temperature. A tentative value of the energy required to planarize the fluorene backbone of (15.6 ± 2.5) kJ mol^{-1} monomer is suggested. The beta phase was found even in extremely dilute solutions, believed to be the result of chain folding or well dispersed aggregates being present from dilution of the original source solutions. PF7, PF8, and PF9 also show beta phase formation in solid spin-cast films. A larger fraction of beta phase was formed in PF7 than PF9 after thermal cycling, in contrast to the solution results, because it is less likely that the close-packed chains in the solid state will allow the formation of planarized chains with the longer PF9 side chains.

5. Experimental

The solutions used in this work were produced by dissolving the solid polyfluorenes ($M_w \sim 200$ kg mol^{-1}) in methylcyclohexane (MCH) and heating the vial in boiling water for approximately 10 minutes to aid dissolution, forming clear solutions. This source solution was then

diluted down with ROMIL ultra-pure MCH through a series of solutions, which were heated at each stage, to reach the required concentration.

The excitation spectra and emission spectra were acquired using a SPEX Fluorolog-3 fluorescence spectrometer using solutions with concentrations of the order of 10 ng mL^{-1}, which provided signals just above the detection limit – of the order of the MCH Raman scattering peak. The integration time was set to 1 second and 3 repeat measurements were averaged, giving a total measurement time of 15 minutes for both the fluorescence and excitation spectra. Each PF sample was cycled from 295 K to ~220 K (or sufficient to induce beta phase formation) then back to 295 K. The fluorescence and excitation spectra were collected alternately in series; 1) at 295 K, 2) at the low temperature, 3) as a function of time after returning to 295 K. The samples were scanned continuously for the duration of the experiment (~1 or 2 days).

The absorption spectra were captured on a Perkin-Elmer Lambda-19 spectrophotometer, using concentrations of the order of 10 μg mL^{-1} and giving an OD ~ 0.4–0.9.

The solution samples in all the measurements were cooled in a Janis Research VNF-100 liquid nitrogen variable temperature cryostat using a quartz cuvette with a 1cm path length, and the temperature was set using a LakeShore Model 332 temperature controller.

The absorption spectra were collected from samples in thermal and conformational equilibrium by monitoring the spectrum as a function of time at each temperature (~3–4 h) until no further changes in the spectra were detected.

Film samples were spin-cast from 10 mg mL^{-1} solutions in MCH onto quartz substrates. The solutions were spun at 500 rpm for 5 s, then 2 500 rpm for one minute.

Acknowledgements

D. W. B. wishes to thank the DTI for funding of the TOPLESS project and Thorn Lighting Ltd. for studentship funding.

Received: March 4, 2008
Revised: October 2, 2008
Published online: December 2, 2008

[1] M. Grell, D. D. C. Bradley, X. Long, T. Chamberlain, M. Inbasekaran, E. P. Woo, M. Soliman, *Acta Polym.* **1998**, *49*, 439.
[2] M. Grell, D. D. C. Bradley, G. Ungar, J. Hill, K. S. Whitehead, *Macromolecules* **1999**, *32*, 5810.
[3] M. J. Winokur, J. Slinker, D. L. Huber, *Phys. Rev. B* **2003**, *67*, 184106.
[4] M. Ariu, M. Sims, M. D. Rahn, J. Hill, A. M. Fox, D. G. Lidzey, M. Oda, J. Cabanillas-Gonzalez, D. D. C. Bradley, *Phys. Rev. B* **2003**, *67*, 195333.
[5] C. Rothe, S. M. King, F. Dias, A. P. Monkman, *Phys. Rev. B* **2004**, *70*, 195213.
[6] A. J. Cadby, P. A. Lane, H. Mellor, S. J. Martin, M. Grell, C. Giebeler, D. D. C. Bradley, M. Wohlgenannt, C. An, Z. V. Vardeny, *Phys. Rev. B* **2000**, *62*, 15604.
[7] S. H. Chen, H. L. Chou, A. C. Su, S. A. Chen, *Macromolecules* **2004**, *37*, 6833.
[8] S. H. Chen, A. C. Su, S. A. Chen, *J. Phys. Chem. B* **2005**, *109*, 10067.
[9] M. Knaapila, V. M. Garamus, F. B. Dias, L. Almasy, F. Galbrecht, A. Charas, J. Morgado, H. D. Burrows, U. Scherf, A. P. Monkman, *Macromolecules* **2006**, *39*, 6505.
[10] M. Knaapila, F. B. Dias, V. M. Garamus, L. Almasy, M. Torkkeli, K. Leppanen, F. Galbrecht, E. Preis, H. D. Burrows, U. Scherf, A. P. Monkman, *Macromolecules* **2007**, *40*, 9398.
[11] M. Brinkmann, *Macromolecules* **2007**, *40*, 7532.
[12] M. H. Rahman, C. Y. Chen, S. C. Liao, H. L. Chen, C. S. Tsao, J. H. Chen, J. L. Liao, V. A. Ivanov, S. A. Chen, *Macromolecules* **2007**, *40*, 6572.
[13] S. Becker, C. Ego, A. C. Grimsdale, E. J. W. List, D. Marsitzky, A. Pogantsch, S. Setayesh, G. Leising, K. Mullen, *Synth. Met.* **2001**, *125*, 73.
[14] M. C. Hung, J. L. Liao, S. A. Chen, S. H. Chen, A. C. Su, *J. Am. Chem. Soc.* **2005**, *127*, 14576.
[15] J. Morgado, L. Alcacer, A. Charas, *Appl. Phys. Lett.* **2007**, *90*, 201110.
[16] H. H. Lu, C. Y. Liu, C. H. Chang, S. A. Chen, *Adv. Mater.* **2007**, *19*, 2574.
[17] F. D. Dias, J. Morgado, A. L. Macanita, F. P. Costa, H. D. Burrows, A. P. Monkman, *Macromolecules* **2006**, *39*, 5854.
[18] W. Chunwaschirasiri, B. Tanto, D. L. Huber, M. J. Winokur, *Phys. Rev. Lett.* **2005**, *94*, 107402.
[19] M. E. Caruso, M. Anni, *Phys. Rev. B* **2007**, *76*, 054207.
[20] C. Rothe, F. Galbrecht, U. Scherf, A. Monkman, *Adv. Mater.* **2006**, *18*, 2137.
[21] W. C. Tsoi, A. Charas, A. J. Cadby, G. Khalil, A. M. Adawi, A. Iraqi, B. Hunt, J. Morgado, D. E. Lidzey, *Adv. Funct. Mater.* **2008**, *18*, 600.
[22] C. C. Kitts, D. A. Vanden-Boot, *Polymer* **2007**, *48*, 2322.
[23] M. Knaapila, L. Almasy, V. M. Garamus, M. L. Ramos, L. L. G. Justino, F. Galbrecht, E. Preis, U. Scherf, H. D. Burrows, A. P. Monkman, *Polymer* **2008**, *49*, 2033.
[24] H. L. Vaughan, F. M. B. Dias, A. P. Monkman, *J. Chem. Phys.* **2005**, *122*, 014902.
[25] M. Miyahara, H. Kawasaki, T. Fukuda, Y. Ozaki, H. Maeda, *Colloids Surf. A* **2001**, *183*, 475.